IOP Conference Series: Materials
Science and Engineering

PAPER • OPEN ACCESS

Analysis of a rotor supported in bearing with gyroscopic effects

To cite this article: Fulaj Deb *et al* 2018 *IOP Conf. Ser.: Mater. Sci. Eng.* **402** 012059

Analysis of a rotor supported in bearing with gyroscopic effects

Fulaj Deb, K Jegadeesan and C Shravankumar*

Department of Mechanical Engineering, M.Tech. (CAD) SRM Institute of Science and Technology, Chennai

* Corresponding author: shravankumar.c@ktr.srmuniv.ac.in

Abstract. Rotors with one or more offset disks and supported on bearings are common in high speed turbomachinery. During start up, these rotors have to cross through several critical speeds before reaching their operating speed. At critical speeds, the spin speed of the rotor matches with one of its natural frequency leading to the condition of resonance and large vibration amplitude. In rotating systems, these natural frequencies depend on the support stiffness. Also, they are a function on the spin speed because of the phenomenon of gyroscopic effect. The gyroscopic effects on critical speeds of a rotor system supported in bearing can be studied by means of a Campbell diagram, which has been used in the design of turbines. In this paper, gyroscopic effects of a rotor with an offset disk and supported on bearing is studied by means of Campbell diagrams. The numerical study is carried out by modelling of the rotor-bearing system using finite element mass, stiffness and gyroscopic matrices. The solution is obtained by solving the assembled equations of motion; following application of geometric boundary conditions and representing the second order differential equations of motion in state-space form. The results of critical speed obtained are compared with those of the results obtained through modal analysis using FE tool (ANSYS). The analysis of the results can be used to extend the study for a multi-disk rotor with different bearing supports.

Keywords: Rotor-Bearing system, Gyroscopic effects, Critical speeds, Campbell diagram, Finite element method

1. Introduction

The uneven distribution of masses in the rotor creates whirl phenomenon which gets tremendous at the critical speeds and creates excessive threat to the bearings. The gyroscopic effects arise from the presence of rotating masses mounted on the rotor and their orientation with respect to the bearing centre line. This, along with the bearing support conditions continuously causes forward and backward whirl phenomenon in the rotor and induces fatigue loading in the bearings.

During rotation, the components undergo continuous precession due to Coriolis force and hence induce gyroscopic effect. The effect produces moments on the rotor which leads to backward whirling and forward whirling of the rotor. The effects in turn on the bearings are fatigue loadings. The consequence of it makes the bearings prone to catastrophic failure and damage to machineries. It is

IOP Conf. Series: Materials Science and Engineering **402** (2018) 012059 doi:10.1088/1757-899X/402/1/012059

therefore very essential to determine the critical speeds of such a rotor so that while running at high speeds, the critical speeds can be avoided or bypass those speeds as quickly as possible.

A rotor shaft with simply supported boundary conditions has been modelled by researchers like Glasgow and Nelson **[1]**, and Lund **[2]**. Similar shaft with hydrodynamic bearing supports has been studied in the works of Kim and Lee **[3]**. Here, the rotor system was modelled as a circular shaft of length 1.27 m and diameter 0.1016 m. Its elastic modulus is 2.068×10^{11} N/m^2 and its density is 7833 kg/m^3. The bearing stiffness and damping parameters are as follows: $k_{yy} = k_{zz} = 1.7513 \times 10^7$ N/m, $k_{yz} = k_{zy} = -2.917 \times 10^6$ N/m, $c_{yy} = c_{zz} = 1.752 \times 10^3$ N-s/m, $c_{yz} = c_{zy} = 0$. The model is discretised in to five finite elements of equal length.

In practice, rotating machineries have multiple disks or blades attached to a flexible/ elastic shaft with variable cross-section. It becomes essential for the engineer to quantify their natural frequencies, critical speeds, vibration modes and their response to different types of excitation. For this purpose, one of the methods used is finite element method.

For analytical convenience, these rotors are often modelled either as a concentrated mass on a massless elastic shaft or as a uniform continuous rotor system. The latter is discussed in this paper.

1.1. Campbell Diagram

The natural frequencies of a rotating shaft are the function of angular velocities, i.e., the shaft spin speed due to two factors. One is due to the gyroscopic effects of rotor system. The other is due to variation of bearing stiffness and damping as a function of spin speed. For the forward whirling modes, their natural frequencies increase with increasing spin speed, while for the backward whirling modes, their natural frequencies decrease. Critical speeds, which occur when the rotor spin-speed matches with its natural frequencies, can be identified by plotting the Campbell diagram.

Pyrhonen et. al. modelled a solid-rotor with two impellers **[4]**. They used a beam finite element which undergoes shear deformation. Four transverse Degrees of Freedom (DoFs) are considered in the model, neglecting the axial and torsional DoFs. Two ball bearings support the rotor. The bearings have unsymmetrical stiffness and damping coefficients. The impellers are modelled as rigid disks mounted on the rotor using translational and rotational springs. Four critical speeds are obtained. One critical speed of a backward whirling mode is slightly excited due to asymmetrical bearing stiffness. Based on the critical speeds obtained, the safe operating speed range for the rotor is decided.

Ku presented a rotor model using finite element method which is used to study the whirl speeds and stability of rotor-bearing systems **[5]**. The finite element model includes: translational and rotary inertia, gyroscopic moments, transverse shear and internal damping (viscous and hysteretic). In the finite element model, Timoshenko beam elements are used. There are three nodes in the finite element and four DoFs are assigned to each node. Damping model is incorporated as a combined effect of both viscous and hysteretic internal damping. A linear bearing model is chosen, with eight stiffness and damping coefficients. Comparison of numerical results with earlier literature checks the accuracy of the developed finite element model. Internal damping leads to rotor instability of forward whirling modes. The backward whirling modes are always stable. It is observed that additional external damping contributed to increasing the onset speed of instability.

Hui et al. **[6]** studied natural frequencies of a typical stepped shaft used in reactor engineering using finite element analysis simulation software (ANSYS). Three different element types have been used to model the rotor shaft, namely, Beam188, Solid273 and Solid186. The results are compared. It is observed that in most cases, modelling using axisymmetric element types can achieve the same accuracy as that using solid element type.

In this paper, two models of a rotor system are discussed: one is a rotating flexible shaft with its bearing support condition as cantilever boundary condition. The other is a rotating flexible shaft with a fixed bearing support and a rigid disc mounted at the end of the shaft. In the following section, a mathematical modelling of the rotor-bearing system is discussed.

2. Mathematical model

The rotor system is modelled as an elastic shaft with uniformly distributed mass and stiffness properties. At one end, it is supported on a bearing and a disk is attached to it at the other end. The disc is modelled as a rigid body. Gyroscopic moments due to the shaft/ disc mass are considered. The bearing is modelled using stiffness and damping elements, which can consider stiffness and damping coefficients in two transverse directions as well as cross-coupled coefficients. Any effect of damping from bearing or due to internal damping is neglected. **Figure 1** shows the model of a flexible shaft with a rigid disc and its DoFs.

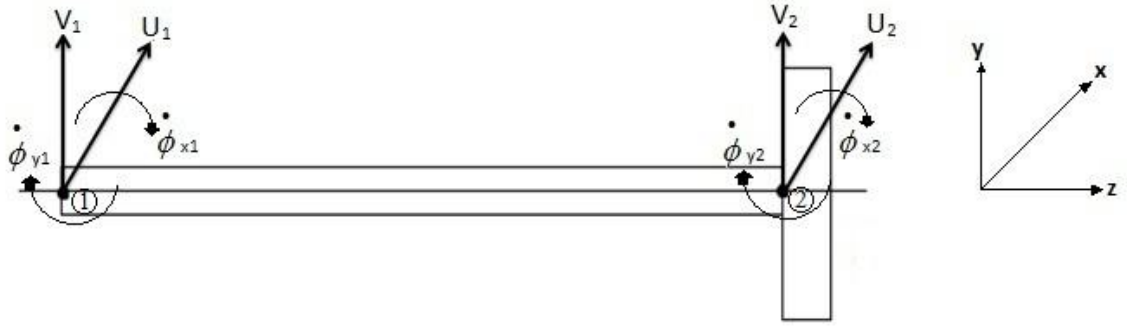

Figure 1. A flexible shaft with a rigid disc.

2.1. Bearing model

Generally, a bearing support is modelled using stiffness and damping coefficients. In a low-speed bearing model these coefficients are constant. But, in a high-speed bearing, these coefficients are a function of the rotor spin-speed. In this paper, a low-speed bearing model is considered with speed independent stiffness coefficients chosen from recent literature (Kurvien et. al. **[7]**), pertaining to the bearing support of a hig h-speed generator model. In this paper, a low-speed bearing model is considered with speed independent stiffness coefficients.

Further, in this paper two numerical problems are presented. In the first model, a rotating shaft is supported on a bearing support which is assumed to provide a fixed end boundary condition, constraining the translational displacements along the two lateral axes and angular displacements about those axes. In the second model, a disc and a bearing support, one at each end of the shaft is modelled and the bearing support is assumed as a fixed end. The parameters of the rotor system are provided in **Table 1.**

Table 1. Parameters of the rotor system.

System parameters	
Shaft length,	$l = 1.5$ m
Shaft radius,	$r = 0.030$ m
Shaft density,	$\rho = 7810$ kg/m^3
Shaft Elastic modulus,	$E = 2\text{x}10^{11}$ N/m^2
Shaft Polar moment of inertia,	$I_p = 0.0048$ kg-m^2
Shaft Area moment of inertia,	$I_a = 3.0680\text{e-}07$ m^4
Disc mass,	$m_d = 0.55206$ kg
Disc mass moment of inertia	$I_d = 0.0031$ kg-m^2
Dic Polar mass moment of inertia	$I_{pd} = 0.0062$ kg-m^2

2.2. Finite element model

In the finite element model, the transverse vibration of the shaft is discretized in to finite elements. The shaft finite elements are modelled based on Euler-Bernoulli beam theory. The finite element is a two node element with four generalized displacements. They are two translational displacements

u and v (along X and Y axes) and two rotational displacements ϕ_y and ϕ_x (about X and Y axes). The rotor model is shown in Fig. 1. The elements are isotropic and symmetric about the longitudinal axis Z. The axi-symmetric geometry of the element results in same mass and stiffness matrices in both the transverse planes. The elemental equations of motion for rigid disk and a flexible rotor can be derived using Lagrange's equation.

Flexible shaft element. The governing equation of motion for a shaft finite element is written in matrix representation as in equation **(1)**.

$$\left[M_s^e\right]\left\{\ddot{U}_s^e\right\}+\left[G_s^e\right]\left\{\dot{U}_s^e\right\}+\left[K_s^e\right]\left\{U_s^e\right\}=\left\{F_s^e\right\} \tag{1}$$

Here, $\left[M_s^e\right]$ is the elemental mass matrix, $\left[G_s^e\right]$ is the elemental gyroscopic matrix, $\left[K_s^e\right]$ is the elemental stiffness matrix, $\left\{U^e\right\}=\left[\begin{matrix} x^i & y^i & \phi_y^i & \phi_x^i & x^{i+1} & y^{i+1} & \phi_y^{i+1} & \phi_x^{i+1}\end{matrix}\right]^T$ (superscripts *i* and *i*+1 are the two nodes of the element) is the displacement vector and $\left\{F^e\right\}$ is the force vector. For the analysis of natural whirl frequencies, the force vector on the right hand side can be neglected, $\left\{F\right\}=0$. Further, $\left[M_s^e\right]=\left[M_s^t\right]+\left[M_s^r\right]$ and is given in **Appendices A1** where μ is the mass per unit length, l is the shaft length and r is its radius.

Rigid disc element. The governing equations of motion for the rigid disk element are written in matrix representation as follows in equation **(2)**.

$$\left[M_d^e\right]\left\{\ddot{U}_d^e\right\}+\left[G_d^e\right]\left\{\dot{U}_d^e\right\}+\left[K_d^e\right]\left\{U_d^e\right\}=\left\{F_d^e\right\} \tag{2}$$

Here, $\left[M_d^e\right]$ is the elemental mass matrix for rigid disk, $\left[G_d^e\right]$ is the elemental gyroscopic matrix, $\left[K_d^e\right]$ is the elemental stiffness matrix for the rigid disk. These are given in **Appendices A2**. $\left\{f_d^e\right\}$ is the elemental force vector (forces acting on a disk such as unbalance or forces from adjacent elements) for the rigid disk. Here, these forces are neglected.

Assembly and Boundary conditions. The shaft is discretised in to five line elements with two nodes. The disc is a single element with its node in the centre. The nodes of the disc and shaft are coinciding. For the bearing stiffness in *x* and *y* directions, linear spring elements have been made use of with two nodes. The nodes of the bearing are fixed at one end and at the other end; they coincide with a node of the shaft element. The system equations of motion after assembly are given as follows in equation **(3)**.

$$\left[M\right]\left\{\ddot{U}\right\}+\left[G\right]\left\{\dot{U}\right\}+\left[K\right]\left\{U\right\}=\left\{F\right\} \tag{3}$$

Here, $\left[M\right]$ is the assembled mass matrix, $\left[G\right]$ is the assembled gyroscopic matrix, $\left[K\right]$ is the elemental stiffness matrix for the rigid disk and $\left\{U\right\}$ is the displacement vector.

3. Numerical simulations

The assembled equations of motion are re-written in state-space form with reduced order and then solved as an eigen-value problem. The eigen values obtained correspond to the whirl frequencies (natural frequencies) of the rotor system. The eigen vector corresponds to the mode shapes. The whirl frequencies are obtained for various spin speeds and plotted in the form of a Campbell diagram. **Figure 2** shows the Campbell diagram for a flexible rotor shaft with a fixed support at one end. **Figure 3** shows the Campbell diagram obtained for a flexible shaft rotor system, with a fixed support at one end and a rigid disc mounted at its other end. The intersection of the whirl frequencies with the straight line representing the equation for whirl frequencies equal to spin speed (i.e., 1x harmonic) gives the critical speeds of the rotor system. Also, the rotor systems have been designed and analysed using ANSYS software. The results obtained are compared in **Figure 4** and **Figure 5**.

IOP Conf. Series: Materials Science and Engineering **402** (2018) 012059 doi:10.1088/1757-899X/402/1/012059

3.1. Simulation results from MATLAB

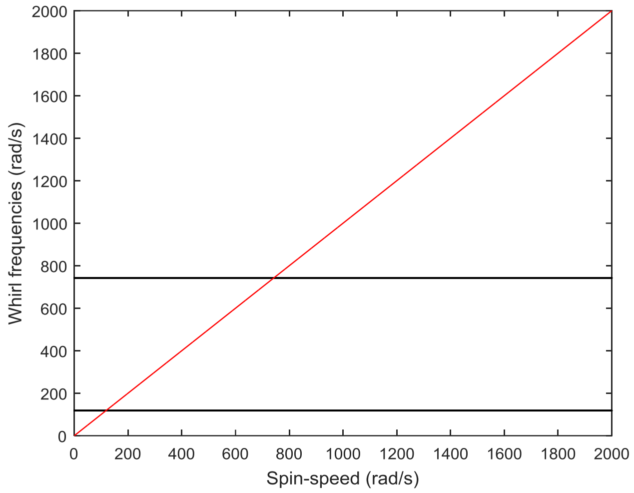

Figure 2. Flexible shaft with a fixed end support.

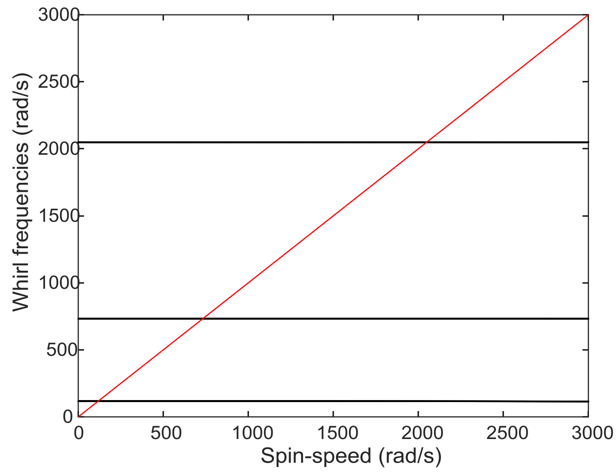

Figure 3. Flexible shaft with rigid disc and a fixed end support.

3.2 Comparison with simulation in ANSYS

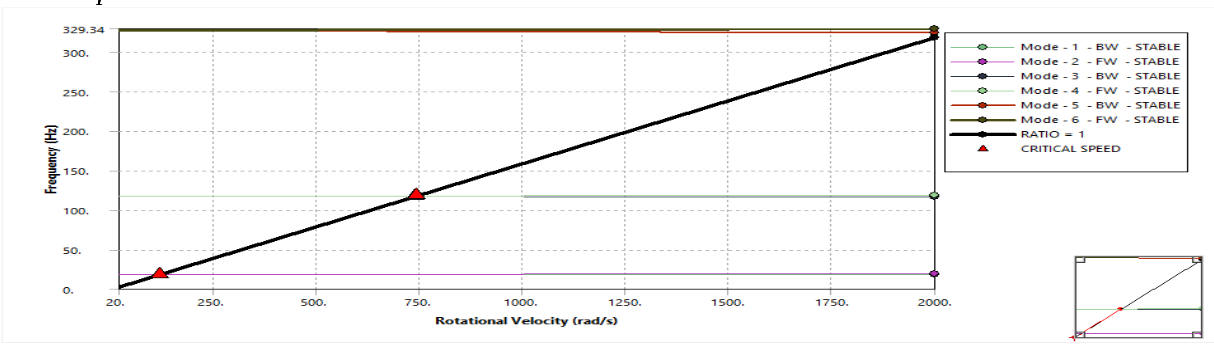

Figure 4. Campbell Diagram for a flexible shaft with fixed end support – ANSYS.

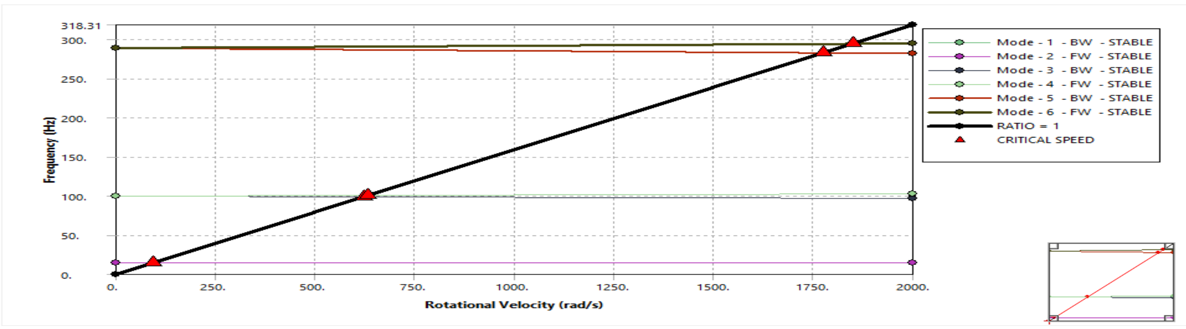

Figure 5. Campbell Diagram for a flexible shaft with a rigid disc and a fixed end support – ANSYS.

IOP Conf. Series: Materials Science and Engineering **402** (2018) 012059 doi:10.1088/1757-899X/402/1/012059

4. Results and Discussion

The critical speeds are obtained from the Campbell diagrams. **Table 2** compares the critical speeds obtained for flexible shaft on a rigid support, obtained from MATLAB and ANSYS results. **Table 3** compares the critical speeds obtained for flexible shaft with rigid disc and rigid support, obtained from MATLAB and ANSYS.

Table 2. Comparison of critical speeds obtained from Campbell plots for flexible shaft on rigid support (FW- Forward whirl, BW – Backward whirl).

Mode shapes	Critical Speed (rad/s)	
	MATLAB	**ANSYS**
1 (FW) 1 (BW)	121	122
2 (FW) 2 (BW)	743	746

Table 3. Comparison of critical speeds obtained from Campbell plots for flexible shaft with rigid disc on a rigid support (FW- Forward whirl, BW – Backward whirl).

Mode shapes	Critical Speed (rad/s)	
	MATLAB	**ANSYS**
1 (FW) 1 (BW)	127	116
2 (FW) 2 (BW)	744	730
3 (FW) 4 (BW)	2057	1850

5. Conclusion

The presented work mainly discusses obtaining the critical speeds for a rotor-bearing system. A mathematical model of flexible shaft with rigid rotor has been developed using finite element methods. The finite element model was used for obtaining critical speeds in MATLAB. The same model was designed and analysed by the FEA tool ANSYS and the critical speeds are compared with the critical speeds obtained from MATLAB. The critical speeds obtained from MATLAB and ANSYS match with one another. This also conforms the validity of the developed finite element model.

Appendices

A-1

$$\left[M_t^s\right]=\frac{\mu l}{420}\begin{bmatrix} 156 & & & & & & & \\ 0 & 156 & & & & sym & & \\ 0 & -22l & 4l^2 & & & & & \\ 22l & 0 & 0 & 4l^2 & & & & \\ 54 & 0 & 0 & 13l & 156 & & & \\ 0 & 54 & -13l & 0 & 0 & 156 & & \\ 0 & 13l & -3l^2 & 0 & 0 & 22l & 4l^2 & \\ -13l & 0 & 0 & -3l^2 & -22l & 0 & 0 & 4l^2 \end{bmatrix}$$

$$\left[M_r^s\right]=\frac{\mu r^2}{120l}\begin{bmatrix} 36 & & & & & & & \\ 0 & 36 & & & sym & & & \\ 0 & -3l & 4l^2 & & & & & \\ 3l & 0 & 0 & 4l^2 & & & & \\ -36 & 0 & 0 & -3l & 36 & & & \\ 0 & -36 & 3l & 0 & 0 & 36 & & \\ 0 & -3l & -l^2 & 0 & 0 & 3l & 4l^2 & \\ 3l & 0 & 0 & -l^2 & -3l^2 & 0 & 0 & 4l^2 \end{bmatrix}$$

$$\left[G_s^e\right]=\frac{\omega\overline{I_p}}{30l}\begin{bmatrix} 0 & & & & & & & \\ -36 & 0 & & & & skewsym & & \\ 3l & 0 & 0 & & & & & \\ 0 & 3l & -4l^2 & 0 & & & & \\ 0 & -36 & 3l & 0 & 0 & & & \\ 36 & 0 & 0 & 3l & -36 & 0 & & \\ 3l & 0 & 0 & -l^2 & -3l & 0 & 0 & \\ 0 & 3l & l^2 & 0 & 0 & -3l & -4l^2 & 0 \end{bmatrix}$$

$$\left[K_s^e\right]=\frac{EI_a}{l^3}\begin{bmatrix} 12 & & & & & & & \\ 0 & 12 & & & sym & & & \\ 0 & -6l & 4l^2 & & & & & \\ 6l & 0 & 0 & 4l^2 & & & & \\ -12 & 0 & 0 & -6l & 12 & & & \\ 0 & -12 & 6l & 0 & 0 & 12 & & \\ 0 & -6l & 2l^2 & 0 & 0 & 6l & 4l^2 & \\ 6l & 0 & 0 & 2l^2 & -6l & 0 & 0 & 4l^2 \end{bmatrix}$$

A-2

$$\left[G_d^e\right]=\begin{bmatrix} 0 & 0 & 0 & 0 \\ 0 & 0 & 0 & 0 \\ 0 & 0 & 0 & I_p \\ 0 & 0 & -I_p & 0 \end{bmatrix} \quad \left\{U_d^e\right\}=\left[x^j \quad y^j \quad \phi_y^j \quad \phi_x^j\right]^T$$

6. References

[1] Glasgow D A and Nelson H D 1979 *J. Mech. Des.* **102** 352
[2] Lund J W 1974 *J. Eng. Ind* **96** 509
[3] Kim Y D and Lee C W 1986 *Journal of Sound and Vibration* **111** 4414
[4] Pyrhonen J, Nerg J, Mikkola A, Sopanen J and Aho T 2009 *Electr Eng* **91** 35
[5] Ku D M 1998 *Mechanical Systems and Signal Processing* **12** 599
[6] Ma H, Zuo H, Tai X and Wen B 2012 *Advanced Engineering Forum* **2-3** 711
[7] Kurvinen E, Sopanen J and Mikkola A 2015 *Mechanism and Machine Theory* **90** 240